JPSE (Journal of Physical Science and Engineering), Vol. 8, No. 1, 2023, Page 76–83.
DOI: 10.17977/um024v8i12023p076

JPSE
(Journal of Physical Science and Engineering)

http://journal2.um.ac.id/index.php/jpse
EISSN: 2541-2485

Optimization of Electro-Optic Sampling by Photodiode's Choice for Terahertz Detection

Fauzul Rizal[1,2*], Imene Benabdelghani[1,2]

[1] Szentágothai Research Centre, Ifjúság street 20, 7624, Pécs, Hungary.
[2] Institute of Physics, University of Pécs, Ifjúság Street 6, 7624, Pécs, Hungary.

***E-mail:** fauzulr@gamma.ttk.pte.hu

Received
23 March 2023

Revised
23 March 2023

Accepted for Publication
24 July 2023

Published
15 January 2024

Abstract
Despite being widely used in a lot of measurements involving the generation of electromagnetic radiation, most of the optimization of this EOS technique only focused on the detection crystal and nonlinear coefficient of the said crystal. After the detection crystal, the combined pump-probe beam should be separated again based on its polarization and measured simultaneously with photodiodes. The authors found out that there are not many studies focusing on this part of the EOS technique and decided to present in this paper to contribute to the better optimization of detection with the EOS technique. We found out that the change of photodiode could have a relationship with the detected signal's shape in the time and space domain, alongside the change of delay-time detection.
Keywords: Electro-optic sampling; photodiode, semiconductor; nonlinear optics.

1. Introduction

The Terahertz band is located between microwaves and the infrared radiation frequency band (from 0.3 THz to 3 THz, corresponding to 1–100 μm wavelength), and it shares some properties with each of these other two electromagnetic radiation. THz radiation is non-ionizing radiation (unless on a very high intensity [1]). The THz band had remained unexplored for a long time due to the lack of useful sources and detectors, making this spectral region often called THz-gap. Science and technologies based on Terahertz (THz) frequency electromagnetic radiation have developed rapidly to the extent that it recently touched many areas from fundamental science to end-user practical applications [2] as the frontier area of the scientific community itself [3]. The main reason for this rapid development lies on the fact that THz radiation can couple resonantly to numerous fundamental motions of proteins, ions, electrons, and electron spins in all phases of matter [4]. Consequently, a wide range of possible implementations of THz technology in various fields, such as imaging, sensing, quality control, wireless communication, biomedicine, and basic science, are gaining notable attention [5]–[9]. This ability of THz radiation that passes through a wide variety of non-conducting materials also makes it an interesting medium to develop better imaging technology as well as material characterization [9], [10].

The advancement of electronics and photonics technology of the THz generation still faces some challenges in generation efficiency and detection. For example, despite the importance of THz radiation and technology, we still lack efficient sources and struggling with a small number of conversion efficiency [11]–[13]. These currently small numbers of conversion efficiency – despite being improved year-by-year – need extra care on the detection side of the experiment.

One of the second-order nonlinear optical processes is optical rectification and difference-frequency generation. In terms of THz generation, these two processes generate photons at a THz frequency ωT by the interaction of two optical photons at frequencies $\omega 1$ and $\omega 2$ within the nonlinear crystal [14]. THz sources based on second-order nonlinear optical effects of optical rectification are being looked into because of their power scalability [15].

Optical rectification (OR) is an alternative mechanism for pulsed THz generation and is based on the inverse process of the electro-optic effect. Optical rectification can be utilized to generate broadband

THz output in a nonlinear optical medium by difference-frequency mixing between pairs of frequency components of the same optical pulse. First demonstrations of this method used picosecond pulses and ZnTe, ZnSe, CdS, and quartz crystals [16], that by the advancement of femtosecond laser, was extended [17], which enabled to generate much broader bandwidths in the THz region. Optical rectification was also demonstrated in zinc-blende type GaAs and GaP crystals [18]–[20], which have much smaller THz absorption. Efficient THz generation by OR requires phase matching, i.e., matching the group velocity of the optical pump pulse to the phase velocity of the THz radiation [21]:

$v_{NIR}=v_{THz}$ …….. (1)

which trivially implied that $n_{gr,NIR}=n_{THz}$. Where $n_{gr,NIR}$ and n_{THz} are group index of near-infrared and refraction index of THz radiation, respectively.

This method needs a careful examination for a velocity matching. Velocity mismatch between the phase velocity of the THz pulse and the group velocity of the probe pulse leading to a reduction of the electro-optic signal measured on the output, thus distort the THz pulse that we needed as illustrated in figure 1, the THz transient and the intensity envelope of the probe pulse are shown at different times (t1 <t2 <t3) while propagating through the crystal. The dashed lines show the intensity envelopes of the probe pulse if there is no velocity mismatch. If there is a velocity mismatch (solid probe pulse envelopes), the probe pulse experiences a different electric field at different positions in the crystal, leading to a reduction of the electro-optic signal.

For phase-matched condition, the efficiency of THz generation by long plane-wave pulses can be described by the following equation [23]:

$$\eta_{\mathrm{THz}} = \frac{2\omega^2 d_{eff}^2 L^2 I}{\varepsilon_0 n_{\mathrm{NIR}}^2 n_{\mathrm{THz}}^2 c^3} exp\left(-\alpha_{\mathrm{THz}}\frac{L}{2}\right)\frac{sinh^2(\alpha_{\mathrm{THz}}(L/4))}{(\alpha_{\mathrm{THz}}(L/4))^2} \quad \text{…….. (2)}$$

Where ω is the angular difference (THz) frequency, d_{eff} is the effective nonlinear coefficient, I the intensity of the near- infrared (NIR) light, $\epsilon_0$is the vacuum permittivity, c is the speed of light in vacuum, L is the length of the nonlinear crystal, α_{THz} is the absorption coefficient for the THz radiation, n_{NIR} and n_{THz} are the refraction indices in the NIR and THz range, respectively. We clearly see that the conversion efficiency in optical rectification depends primarily on the material's nonlinear coefficient and the phase-matching conditions.

Currently, the most popular setup to detect THz generation due to the versatility and flexibility to adapt in any experiment in optics and spectroscopy by the means called electro-optic sampling (EOS) [24]–[27]¬. EOS is an optoelectronic technique of optical sampling, which exploits the linear electro-optic effect. When ultrashort optical pulses are used in the electro-optic probe, there is only a short time interval in which the electric field at the probe can influence the light. This makes a change in polarization, which is turned into a change in optical power at a polarizer – can then be measured without requiring a very fast photodetector [28].

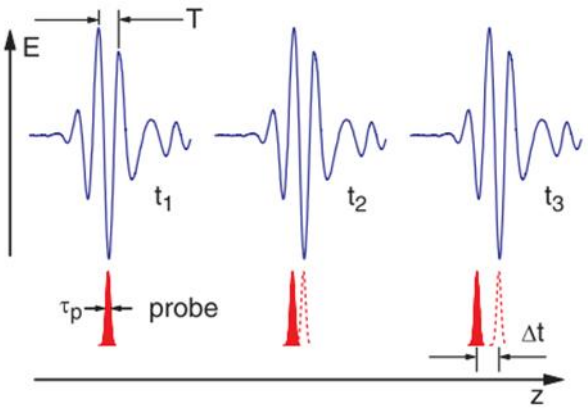

Figure 1. Effect of a velocity mismatch [22]

A full waveform of a periodic signal can then be obtained by slowly varying the delay of the probe pulse, i.e., by sequential sampling of a repetitive signal. For each setting of the relative time delay, the signal obtained can be average¬d over many pulses, so that noise is averaged out and a very high sensitivity is achieved. Most basic technique is utilizing balanced detection with two photodetectors and lock-in detection with a modulated trigger. Such techniques make it possible to achieve a sub-millivolt resolution within a measurement time of 1 s [29], even though the half wave voltage of the electro-optic probe is typically in the kilovolt region. EOS uses pump–probe systems, that use two copies of optical pulse which one of them propagate with a variable time delay, controlled with an adjustable optical delay line. Mechanically changing the time delay allows sequential sampling of different portions of a waveform. There are at least two types of common probe for EOS, direct- and indirect EOS. In direct EOS, an electro-optic material should be used as a substrate as the electro-optic medium. Some of these materials are GaAs, InP, ZnTe, and GaP. While in external EOS, one uses an external electro-optic probe. This probe may be a plate of electro-optic material, either used in transmission or reflection, or a small crystal with nanostructure, which may be mounted on a fibre. Often used nonlinear crystal materials are lithium tantalate ($LiTaO_3$) or bismuth silicate (BSO).

EOS have much more benefits compared to other detection and characterization method. EOS allows the complete characterization of the electric field using a second-order nonlinear process and has widely applied to field metrology for frequencies ranging from a few THz through the mid- and near-IR [28]. EOS is easy to implement since it does not require a vacuum environment. Other conventional techniques based on photoionization or photoemission have also shown promise for the detection of fields in the visible range [30]–[32], however for the detection of weak fields, however, the sensitivity and dynamic range of EOS make it an attractive approach [33], where techniques such as balanced detection can cancel technical noise from the laser. More importantly in THz generation, EOS could measure huge band of sampling generated by the crystal with independent response of the carrier-envelope pulse of the sampling pulse [28]. Based on a second-order nonlinear effect, EOS is well described by the nonlinear wave equation. Because the EOS response function is independent of the carrier-envelope pulse of the sampling pulse, allowing for the characterization of fields across all adjustable parameters without affecting the detection. This feature makes EOS as conveniently easy-to-implement technique for sampling generated THz electric fields.

Despite being widely used in a lot of measurements involving generation of electromagnetic radiation, most of optimization on this EOS technique only focused on the detection crystal and nonlinear coefficient of the said crystal. While after the detection crystal the combined pump-probe beam should be separated again based on its polarization and measured simultaneously with photodiodes. Authors found out that there are not many studies focusing on this part of EOS technique and decided to present in this paper to contributing to the better optimization of detection with EOS technique for the scientific community

2. Method

2.1 Experimental setup

We are using the standard EOS setup fed by a 1030 nm femtosecond laser on a 1 kHz repetition rate and 1 mJ pulse energy. GaP and ZnTe were chosen as the favorable generating- and detecting-crystal (respectively) in this letter owing to its high electro-optic coefficient, and its relatively small dielectric constant (reducing back action on the sample). The invasiveness of electro-optic probes is often a considerable concern, as the use of an electro-optic probe with a high dielectric constant can cause time delays and reflections in the device under test [34]. The EOS setup used for this experiment is shown in Figure 2.

The input beam is being split with TFP for pump and probe purposes. A sum of the total distance traveled by both pump and probe should be equal at the initial delay stage position (shown in the blue box) to ensure that both beams arrive at the same phase on the EO crystal. The pump beam, which is vertically polarized entered the GaP (110) crystal and interacting nonlinearly to generate THz radiation by optical rectification. Both pump and probe beams later met inside ZnTe (100) as the EO crystal and being sent to the later stage of detection. The residual beams which are not needed are blocked by iris and the noise is reduced by neutral density (ND) filter. The last stage is to separate two polarizations of the beam by Wollaston prism and adjusting the optimum intensity with quarter-wave plate to ensure that the beam intensity for both polarizations will not exceed the threshold level and saturating the

photodiodes (PD) in the ends. Signal is obtained by mechanically control the movement of delay stage from ±0.5 cm back and forth from its initial position. This experiment is repeated by changing the type photodiodes in the end while maintaining all parameters to be controlled

2.2 Instruments and Parameters Used

Four types of semiconductor photodiodes are being collected for this measurement: A pair of InGaAs (Thorlabs® DET10C/M) photodiode, a pair of Si (Thorlabs® DET10A/M) photodiode, a pair of Ge (Thorlabs® DET50B/M) photodiode, and another balanced Ge compact photodiode (New Focus® 2317). The responsivity for each photodiode are 0.7 A/W, 0.2 A/W, 0.5 A/W, and 0.4 A/W for InGaAs, Si, Ge, and balanced Ge, respectively [35]. Since the measured beam radius is much less than the active area of all photodiodes used in this letter, we can neglect the difference between active area for each photodiode.

As EOS measurement requires lock-in amplification, we set the lock-in parameter as follows for any photodiode used (InGaAs, Si, Ge, Ge-balanced): 500 Hz repetition rate with sampling time constant 300 ms (in Lock-in). We use ND0.5 filter for all cases in probe line (except for Ge using ND0.5+ND2.0 due to the low saturation level of Germanium) to reduce the intensity of the beam and filtering noises, and long-pass filter to block wild 1.03 micron's reflected/diffracted beam on both photodiode.

3. Result and Discussion

Terahertz measurement with the EOS technique has been done with measured lowest signal-to-noise ratio of 1.65%. The corresponding results for each photodiode and their respective measured signal in both time and spectral domain are shown in Figure 2.

In the time domain, each measurement with different photodiodes shows a slightly different signal. We present the time axis deliberately at the same scale and range in Figure 2, so that the difference of signal delay response could be immediately observed. InGaAs photodiodes showed the lowest time-shift delay detection and compact Ge showed the biggest time-delay detection. InGaAs photodiodes have typically around 10 ns response time, while Germanium has a 500-1000 ns time and Silicone have 10-20 ns typical response time [35]. Resulting InGaAs signal read comes first compare to Germanium signal reads. The balanced-Ge photodiodes deviding the signal electronically from two different detection surface at once before sending response to the computer. We suspect that this might case on the late response time compared to the separate pair of Ge photodiodes. While spatially giving advantages for the setup, balanced photodiodes could have slower time response to the signal in which could not be negligible in the attosecond physics. As we can clearly see from the measured data, the choice of semiconductor photodiodes with appropriate response time plays an important rule on where we could find the signal on the time domain.

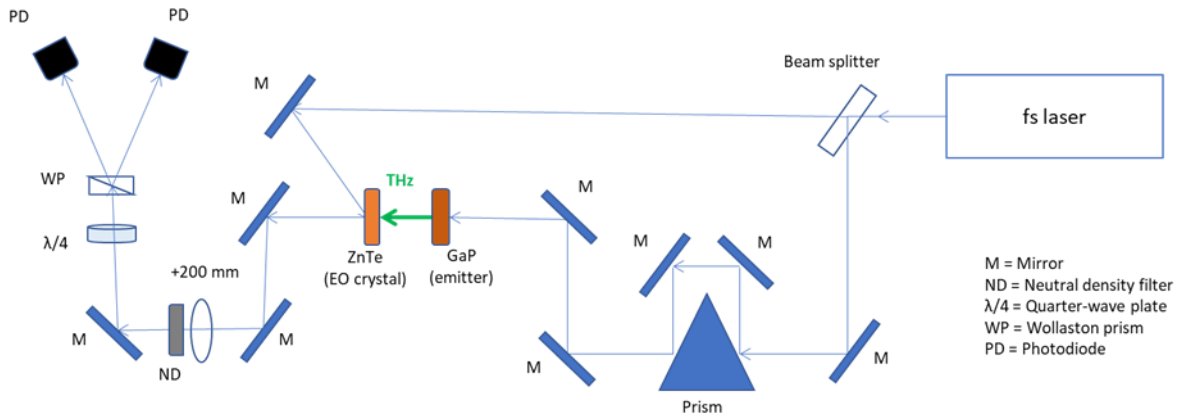

Figure 2. Electro-optic sampling used in this letter.

In the frequency domain, in which solely relied on the pulse shape on the time domain itself, we can see that there are no particular difference between the choice of photodiodes. All measurements shows a bandwith of 4 THz read. However the shape of the pulse in the time domain shows the high asymetric tendency for InGaAs and slightly asymetric tendency in Ge photodiodes (both compact and separate pair). Silicone photodiodes, on the other hand, shows a very nice symetrical pulse shape compare with the other. While the pulse shaping can also be done mainly by adjusting the intensity difference between two beams after the Wollaston prism, in this letter we make sure that the intensity of both beams are adjusted in the same way for every measurement. Even with the spatial and angular optimization of the setup and the photodiodes itself, InGaAs always showed the tendency to read an uneven cycle of THz pulse. Leads to the conclusion that even though it gives the hghest peak-to-peak signal voltage, it might be a disadvantage if one tries to study the pulse shape throughoutly.

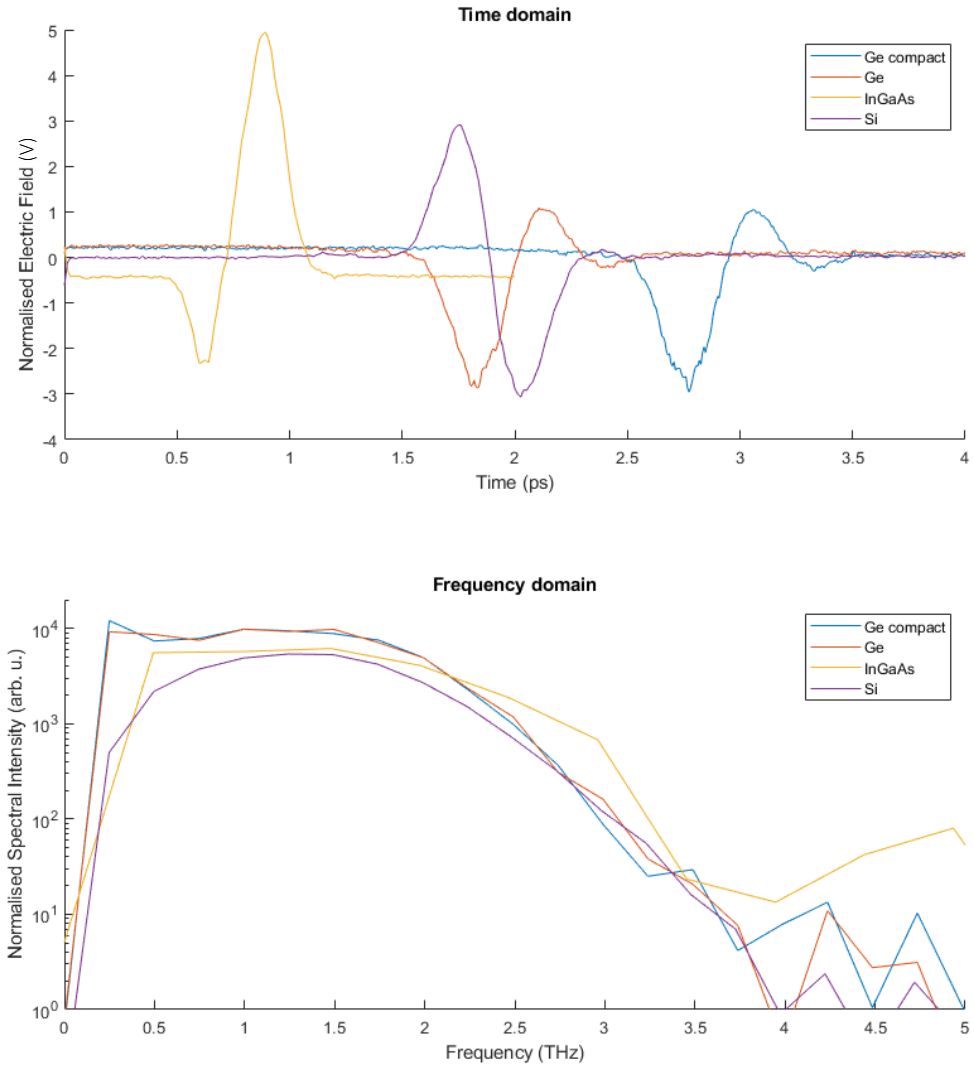

Figure 3. EOS measurement result using different types of photodiodes both in time and frequency domain.

The strength of the signal could be easily compare by normalize the central part of the pulse in space and compare the signal shapes and peaks in a single graph, as shown in figure 3. As we expected, the same type of semiconductor for photodiodes showed an almost similar shape of signal obtained. Measurement with InGaAs photodiode showing highest peak-to-peak value of 7.28 Volt. Silicone, Germanium, and Germanium-compact photodiodes are showing 6.02, 4.59 V, and 5.17 V peak-to-peak signal value, respectively. In a near-field applications, where ones should work with smallest pump intensity as possible to not damage the generating crystal, InGaAs could give an advantage to be more sensitive with the signal readings. However as mentioned before, the signal shape obtained with InGaAs is not the best compare with the other. This is true even in the spatial regime. Germanium photodiodes on the other hands showed noisy signal despite being treated with stronger filter because of their lower cut-off voltage (5 V) compare with the others (InGaAs and Si have 10 V cut-off voltage). This could also because of the sensitivity of Ge photodiodes which can work in notably large wavelength range (800 – 1800 nm) compared with the others (Silicone have responsivity between 200 – 1100 nm, InGaAs have responsivity between 800 – 1550 nm) [35]. Some wild reflections and wild scattered far-infrared could also interfered with the signal read of Ge photodiodes that naturally filterred out with the other photodiodes. The lowest signal-to-noise ratio obtained comes from Si photodiode with only 0.48% measured in this letter. Followed by Ge with 1.01%, Ge-compact with 1.5%, and InGaAs with 1.65% signal-to-noise ratio. The data of all abovementioned measurements and comparison parameters are summarized in the table 1.

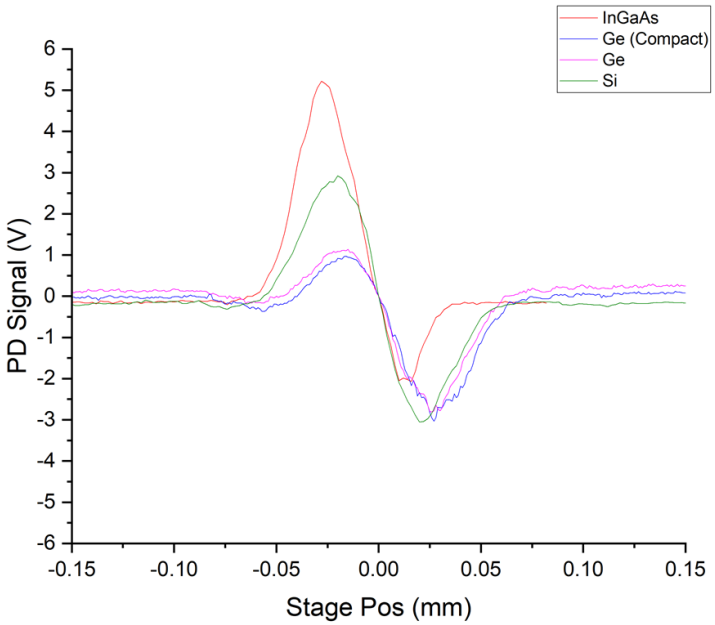

Figure 4. Normalized measured signal in the space-domain (represented by the stage position).

Tabel 1. The type and size of the font used in the article.

Parameter	InGaAs	Si	Ge	Ge-compact
Peak-to-peak voltage	7.28 V	6.02 V	4.59 V	5.17 V
Signal-to-noise ratio	1.65%	0.48%	1.01%	1.50%
Delay time detection	0.5 ps	1.5 ps	1.5 ps	2.5 ps
Bandwidth	4 THz	4 THz	4 THz	4THz
Time-domain pulse shape	Asymmetric	Symmetric	Symmetric	Symmetric
Space-domain pulse-shape	Asymmetric	Symmetric	Almost symmetric	Almost symmetric

4. Conclusion

Terahertz measurement with EOS technique has been done with InGaAs photodiodes showing the lowest time-shift delay detection and compact Ge showed the biggest time-delay detection, while in the frequency domain there are no particular difference between the choice of photodiodes. The shape of the pulse both in in the time and space domain shows the high asymetric tendency for InGaAs and a really good symmetric signal shape from Si photodiode. While InGaAs have this asymmetrical signal-shape tendency, it gives the most sensitive signal readings. Makes it a better choice to work with low-

energy field. The best signal shape and noise-to-signal ratio could be observed in Si photodiodes amongst the other makes this type of photodiode is better if one needed to focus on signal analysis.

References

[1] B. Ewers et al., "Ionization of coherent excitons by strong terahertz fields," Phys. Rev. B - Condens. Matter Mater. Phys., vol. 85, no. 7, pp. 1–5, 2012, doi: 10.1103/PhysRevB.85.075307.

[2] S. S. Dhillon et al., "The 2017 terahertz science and technology roadmap," J. Phys. D. Appl. Phys., vol. 50, no. 4, p. 043001, Feb. 2017, doi: 10.1088/1361-6463/50/4/043001.

[3] A. Irizawa, S. Lupi, and A. Marcelli, "Terahertz as a Frontier Area for Science and Technology," Condens. Matter, vol. 6, no. 3, p. 23, Jun. 2021, doi: 10.3390/condmat6030023.

[4] J. A. Fülöp, S. Tzortzakis, and T. Kampfrath, "Laser-Driven Strong-Field Terahertz Sources," Advanced Optical Materials, vol. 8, no. 3. Wiley-VCH Verlag, Feb. 01, 2020. doi: 10.1002/adom.201900681.

[5] L. Afsah-Hejri, E. Akbari, A. Toudeshki, T. Homayouni, A. Alizadeh, and R. Ehsani, "Terahertz spectroscopy and imaging: A review on agricultural applications," Comput. Electron. Agric., vol. 177, no. September 2019, p. 105628, 2020, doi: 10.1016/j.compag.2020.105628.

[6] Y. Peng, C. Shi, Y. Zhu, M. Gu, and S. Zhuang, "Terahertz spectroscopy in biomedical field: a review on signal-to-noise ratio improvement," PhotoniX, vol. 1, no. 1, pp. 1–18, 2020, doi: 10.1186/s43074-020-00011-z.

[7] J. Xie et al., "A review on terahertz technologies accelerated by silicon photonics," Nanomaterials, vol. 11, no. 7, 2021, doi: 10.3390/nano11071646.

[8] B. Ferguson and X.-C. Zhang, "Materials for Terahertz Optical Science and Technology," Adv. Opt. Mater., vol. 8, no. 3, p. 1901984, Feb. 2002, doi: 10.1002/adom.201901984.

[9] G. Valušis, A. Lisauskas, H. Yuan, W. Knap, and H. G. Roskos, "Roadmap of Terahertz Imaging 2021," Sensors, vol. 21, no. 12, p. 4092, Jun. 2021, doi: 10.3390/s21124092.

[10] B. Zhang et al., "1.4-mJ High Energy Terahertz Radiation from Lithium Niobates," Laser Photonics Rev., vol. 15, no. 3, p. 2000295, Mar. 2021, doi: 10.1002/lpor.202000295.

[11] T. Tanabe, K. Suto, J. Nishizawa, K. Saito, and T. Kimura, "Tunable terahertz wave generation in the 3- to 7-THz region from GaP," Appl. Phys. Lett., vol. 83, no. 2, pp. 237–239, 2003, doi: 10.1063/1.1592889.

[12] G. Polonyi et al., "Highly efficient scalable semiconductor terahertz sources," Int. Conf. Infrared, Millimeter, Terahertz Waves, IRMMW-THz, vol. 2019-Septe, pp. 1–3, 2019, doi: 10.1109/IRMMW-THz.2019.8874482.

[13] B. Zhang et al., "1.4-mJ High Energy Terahertz Radiation from Lithium Niobates," Laser Photonics Rev., vol. 15, no. 3, Mar. 2021, doi: 10.1002/lpor.202000295.

[14] Y. S. Lee, Principles of terahertz science and technology. Springer, 2009. doi: 10.1007/978-0-387-09540-0.

[15] P. S. Nugraha, "Investigation of Scalable Concepts for Intense Terahertz Pulse Generation," University of Pécs, 2020. [Online]. Available: https://mailman.kfki.hu/sympa/arc/fizinfo/2019-12/msg00004/Thesis_Priyo_Print.pdf

[16] T. Yajima and N. Takeuchi, "Far-lnfrared Difference-Frequency Generation by Picosecond Laser Pulses," Jpn. J. Appl. Phys., vol. 9, no. 11, pp. 1361–1371, 1970, doi: 10.1143/JJAP.9.1361.

[17] L. Xu, X. C. Zhang, and D. H. Auston, "Terahertz beam generation by femtosecond optical pulses in electro-optic materials," Appl. Phys. Lett., vol. 61, no. 15, pp. 1784–1786, 1992, doi: 10.1063/1.108426.

[18] M. Nagai et al., "Generation and detection of terahertz radiation by electro-optical process in GaAs using 1.56 μm fiber laser pulses," Appl. Phys. Lett., vol. 85, no. 18, pp. 3974–3976, 2004, doi: 10.1063/1.1813645.

[19] G. Chang, C. J. Divin, C.-H. Liu, S. L. Williamson, A. Galvanauskas, and T. B. Norris, "Power scalable compact THz system based on an ultrafast Yb-doped fiber amplifier," Opt. Express, vol. 14, no. 17, p. 7909, 2006, doi: 10.1364/oe.14.007909.

[20] J. Hebling et al., "Velocity matching by pulse front tilting for large-area THz-pulse generation References and links," Opt. Express, vol. 10, no. 21, p. 299, 2002.

[21] J. A. Fülöp, L. Pálfalvi, G. Almási, and J. Hebling, "Design of high-energy THz sources based on optical rectification," Proc. - TERA-MIR 2009, NATO Adv. Res. Work. Terahertz Mid Infrared Radiat. Basic Res. Pract. Appl., vol. 18, no. 12, pp. 21–22, 2009, doi: 10.1109/TERAMIR.2009.5379649.
[22] K. Reimann, "Table-top sources of ultrashort THz pulses," Reports Prog. Phys., vol. 70, no. 10, pp. 1597–1632, Oct. 2007, doi: 10.1088/0034-4885/70/10/R02.
[23] J. Hebling, K.-L. Yeh, M. C. Hoffmann, B. Bartal, and K. A. Nelson, "Generation of high-power terahertz pulses by tilted-pulse-front excitation and their application possibilities," J. Opt. Soc. Am. B, vol. 25, no. 7, p. B6, Jul. 2008, doi: 10.1364/josab.25.0000b6.
[24] P. Sulzer et al., "Determination of the electric field and its Hilbert transform in femtosecond electro-optic sampling," Phys. Rev. A, vol. 101, no. 3, pp. 1–17, 2020, doi: 10.1103/PhysRevA.101.033821.
[25] B. Crockett, J. van Howe, N. Montaut, R. Morandotti, and J. Azaña, "High-Resolution Time-Correlated Single-Photon Counting Using Electro-Optic Sampling," Laser Photonics Rev., vol. 16, no. 10, 2022, doi: 10.1002/lpor.202100635.
[26] Y. Shang et al., "Polarization determination based on the longitudinal field of a converging terahertz wave," Opt. Lett., vol. 43, no. 22, p. 5508, 2018, doi: 10.1364/ol.43.005508.
[27] X. Wang, Y. Shang, and Y. Zhang, "Polarization characterization by the longitudinal component of a focused terahertz field," Opt. InfoBase Conf. Pap., vol. Part F140-, no. 2018, p. 1, 2019.
[28] E. Ridente et al., "Electro-optic characterization of synthesized infrared-visible light fields," Nat. Commun., vol. 13, no. 1, 2022, doi: 10.1038/s41467-022-28699-6.
[29] Q. Wu and X. C. Zhang, "Free-space electro-optic sampling of terahertz beams," Appl. Phys. Lett., vol. 67, no. 1995, p. 3523, 1995, doi: 10.1063/1.114909.
[30] A. S. Wyatt et al., "Attosecond sampling of arbitrary optical waveforms," Optica, vol. 3, no. 3, p. 303, Mar. 2016, doi: 10.1364/OPTICA.3.000303.
[31] K. T. Kim et al., "Petahertz optical oscilloscope," Nat. Photonics, vol. 7, no. 12, pp. 958–962, 2013, doi: 10.1038/nphoton.2013.286.
[32] S. Sederberg et al., "Attosecond optoelectronic field measurement in solids," Nat. Commun., vol. 11, no. 1, pp. 1–8, 2020, doi: 10.1038/s41467-019-14268-x.
[33] I. Pupeza et al., "Field-resolved infrared spectroscopy of biological systems," Nature, vol. 577, no. 7788, pp. 52–59, 2020, doi: 10.1038/s41586-019-1850-7.
[34] F. Rizal, G. Polónyi, and J. Hebling, "Comparative Study of Semiconductors for Terahertz Generation by Nonlinear Optical Process," XX. Szentágothai János Multidiszcip. Konf. és Hallg. Vers. Absztrakt kötet, p. 215, Mar. 2022, doi: 10.48550/arxiv.2303.05569.
[35] Thorlabs, "Free-Space Biased Detectors," 2023. https://www.thorlabs.com/newgrouppage9.cfm?objectgroup_id=1295